Heliyon

Received:
11 July 2017
Revised:
19 March 2018
Accepted:
5 April 2018

Cite as: Takuma Maruyama, Yoichiro Abe, Takako Niikura. SENP1 and SENP2 regulate SUMOylation of amyloid precursor protein. Heliyon 4 (2018) e00601. doi: 10.1016/j.heliyon.2018.e00601

SENP1 and SENP2 regulate SUMOylation of amyloid precursor protein

Takuma Maruyama [a], **Yoichiro Abe** [b], **Takako Niikura** [a,*]

[a] *Department of Information and Communication Sciences, Faculty of Science and Technology, Sophia University, Japan*

[b] *Department of Pharmacology, Keio University School of Medicine, Japan*

[*] Corresponding author.

E-mail address: niikura@sophia.ac.jp (T. Niikura).

Abstract

Amyloid β, a key molecule in the pathogenesis of Alzheimer's disease (AD), is produced from amyloid precursor protein (APP) by the cleavage of secretases. APP is SUMOylated near the cleavage site of β-secretase. SUMOylation of APP reduces amyloid β production, but its regulatory system is still unclear. SUMOylation, a modification at a lysine residue of a target protein, is mediated by activating, conjugating, and ligating enzymes and is reversed by a family of sentrin/SUMO-specific proteases (SENPs). Here, we found that both SENP1 and SENP2 induced de-SUMOylation of APP. Using quantitative PCR, we also found that expression of SENP1 but not SENP2 increased in an age-dependent manner only in female mice. The results of immunoblot analyses showed that the protein expression was consistent with the PCR results. Females, compared to males, have a higher incidence of AD in humans and show more aggressive amyloid pathology in AD mouse models. Our results provide a clue to understanding the role of SUMOylation in the sex difference in AD pathogenesis.

Keywords: Neuroscience, Cell biology

https://doi.org/10.1016/j.heliyon.2018.e00601

1. Introduction

SUMOylation is a process that post-translationally modifies lysine residues of target proteins by conjugating a small ubiquitin-like modifier (SUMO) to them. The consequences of SUMOylation vary depending on the target proteins, including changes in subcellular localization, sensitivity to other modifications such as ubiquitination, and interaction with other proteins. SUMOylation is a three-step process mediated by enzymes termed E1, E2, and E3. SUMO is activated by the E1 enzyme, a heterodimer of SUMO-activating enzyme subunit -1 and -2, and is then transferred to the SUMO-specific E2 enzyme Ubc9, which conjugates SUMO to target proteins. E3 ligases mediate substrate recognition and SUMO conjugation, although Ubc9 is sufficient in some cases [1]. Protein inhibitor of activated STAT (PIAS) family proteins function as SUMO E3 ligases. SUMOylation is also regulated by SUMO isopeptidases, which are deSUMOylation enzymes that remove SUMOs from target proteins. Six sentrin/SUMO-specific protease (SENP) family proteins (SENP1-3 and SENP5-7) have been identified as SUMO isopeptidases in humans [2]. These proteins primarily localize in the nucleus, but SENP1 and 2 are also present in extranuclear compartments and the cytoplasm [1]. In the SUMOylation pathway, SENPs have three roles, maturation, deconjugation, and chain-editing of SUMO proteins [3]. SENPs remove amino acids after a di-glycine motif in the C-terminal of SUMO proteins (maturation), which enables SUMOs to be conjugated to the lysine residue in substrates. SENP1, 2, 3, and 5 deconjugate SUMOs from the substrates (deconjugation), whereas SENP6 and 7 primarily deconjugate SUMOs from poly-SUMOylated chains (chain-editing). Genetic inactivation of SENP1 or SENP2 leads to embryonic lethality with abnormalities of the brain and heart [4, 5]. Recent studies suggested that SENP1 and SENP2 have neuroprotective functions. The overexpression of SENP1 attenuates ischemia/reperfusion-induced apoptosis [6], and the disruption of neuronal SENP2 induces neurodegeneration [7].

In the central nervous system, protein SUMOylation has been implicated in physiological synaptic function and in the pathogenesis of several neuronal diseases [1, 8]. In Huntington's disease, SUMOylation of Huntingtin protein enhances cytotoxic effects [9]. In amyotrophic lateral sclerosis, superoxide dismutase 1 (SOD1) is SUMOylated by SUMO1 and SUMO2/3 [10,11]. SUMO3 promotes the aggregation of familial disease-linked mutant SOD1, thus leading to cytotoxicity [11]. In Alzheimer's disease (AD), amyloid precursor protein (APP) and tau, the proteins responsible for the pathological hallmarks of AD, amyloid plaques and neurofibrillary tangles, respectively, are both SUMOylated [12, 13, 14, 15]. Tau is primarily modified by SUMO1 at Lys340 located in a microtubule-binding repeat. SUMOylation of tau competes with ubiquitination and is influenced by tau phosphorylation [15]. The relevance of tau SUMOylation in AD pathogenesis is still unclear. APP is cleaved by two enzymes, β- and γ-secretase, and produces amyloid β (Aβ). Aβ is a

https://doi.org/10.1016/j.heliyon.2018.e00601

major component of amyloid plaques and plays a central role in the pathogenesis of AD. SUMOylation of APP at Lys587 and Lys595, which are near the cleavage site of β-secretase, decreases Aβ production [16]. Studies on the global alteration in SUMOylation have shown conflicting results about amyloidogenesis. The global suppression of SUMOylation by RNAi-mediated SUMO down-regulation had no effect on amyloidogenic APP processing, whereas up-regulation of Ubc9, the SUMO E2 ligase, increased APP SUMOylation and decreased Aβ production [14]. Thus, clarifying the regulatory system of APP SUMOylation is important for understanding the role of SUMOylation in Aβ production from APP.

There are sex differences in the development and progression of AD. Multiple studies have suggested that women have a higher AD incidence in old age and generally show a severer progression of cognitive impairment than men [17]. In AD mouse models overproducing Aβ, female 3xTg-AD mice (transgenic mice harboring APPswe, tauP310L, and PS-1M146V) show more aggressive amyloid pathology than male [18], and female 5xFAD mice (transgenic mice harboring APPSwFlLon and PSEN1:M146L*L286V) show a higher Aβ production than males at a young age [19]. Furthermore, behavioral stress increases amyloid burden in female 5xFAD mice but not in males [20]. These results indicate that AD mouse models show sex differences in amyloid-associated AD pathogenesis. However, the molecular mechanism underlying the sex differences is mostly unknown. In this study, we identified SENP proteins that regulate APP SUMOylation as deSUMOylation enzymes and analyzed the expression levels of these SENPs in brains of wild-type and 5xFAD mice.

2. Materials and methods

2.1. Plasmids

Human APP695 cDNA was amplified by RT-PCR from the total RNA of SH-SY5Y cells using primers 5′-GATATCGCCATGCTGCCCGGTTTGGCACTG-3′ and 5′-GCGGCC GCTTTTTGATGATGAACTTCATATCC-3′ and cloned into a pGEM-T vector. The sequence was confirmed, and the cDNA was transferred to a pFLAG-CMV-5a vector between *Hind*III and *Not*I sites. Plasmids containing SENP genes, FLAG-SENP1, FLAG-SENP2, and RGS-SENP3, were obtained from Edward Yeh (Addgene plasmid # 17357, 18047, 18048, respectively) [5, 21, 22]. For the construction of the His-tagged SENP-expressing plasmids, the SENP1 and SENP2 genes were inserted into the pEF4-His(B) vector between *Bam*HI and *Eco*RV sites and between *Eco*RI and *Xba*I sites, respectively. The SENP3 gene was inserted into the pEF4-His(C) vector between *Bam*HI and *Xba*I sites. Plasmids expressing HA-tagged SUMO1/2 were described in Niikura et al. [11].

https://doi.org/10.1016/j.heliyon.2018.e00601

2.2. Cell culture, transfection, and immunoprecipitation (IP)

HEK293 cells were cultured in Dulbecco's modified Eagle's medium (D-MEM) supplemented with 10% fetal bovine serum (FBS), 50 units/ml of penicillin, and 50 μg/ml of streptomycin (Thermo Scientific, Waltham, MA, USA). Cells (1×10^6 cells/dish) were seeded into 60-mm dishes and transfected with plasmids expressing FLAG-tagged APP, HA-tagged SUMO1/2, and His-tagged SENP by lipofection (Lipofectamine 3000, Thermo Scientific). The plasmid DNAs were mixed in a ratio of 3:1:1 for APP:SUMO:SENP. Immunoprecipitation was performed as described in Niikura et al. [11]. Briefly, after 48 h of transfection, cells were lysed in 500 μl RIPA buffer [10 mM sodium phosphate pH 7.2, 150 mM NaCl, 1% Triton X-100, 0.1% SDS, 1% sodium deoxycholate, 10 mM N-ethylmaleimide (NEM), and protease inhibitors (Sigma, St. Louis, MO, USA)]. After the cell lysate was clarified by centrifugation, the protein concentration was measured by BCA protein assay (Thermo Scientific). Then, 20 μl of anti-FLAG M2 antibody-conjugated beads (Sigma) were added to the lysate (approximately 400 μg protein), and the lysate-beads mixtures were incubated at 4 °C for 5 h. The beads were washed with 400 μl RIPA buffer 4 times, and after the buffer was removed, the beads were mixed with 20 μl of 2xsample buffer (125 mM Tris-HCl, 6 w/v% SDS, 15% glycerol, 0.01 w/v% bromophenol blue, 100 mM dithiothreitol) and boiled. Finally, 10 μg of input samples and 20 μl of IP samples were analyzed by immunoblot.

2.3. Animals

All studies involving animals are reported in accordance with the ARRIVE guidelines for reporting experiments involving animals. C57BL6/JJcl (CLEA Japan, Inc. Tokyo, Japan) and AD model mice overexpressing Aβ42, B6-Cg-Tg (APPSwFlLon, PSEN1:M146L*L286V) 6799Vas (5xFAD, Mutant Mouse Resource and Research Center) were used [15]. The mice were housed in polycarbonate cages (3−4 animals per cage) at 22−24 °C under a 12-h light/12-h dark cycle with food and water *ad libitum*. All animal care and experimental procedures complied with the Guidelines for the Care and Use of Laboratory Animals of Keio University and were approved by the Keio University Animal Ethics Committee (09084-8). C57BL6/JJcl (CLEA Japan) mice, whose brains were used for immunoblot analyses, were also housed in the animal facility at Sophia University and the experimental procedures were approved by the Institutional Animal Experiment Committee at Sophia University.

2.4. Brain sample preparation for immunoblot analysis

For the comparison of ages, whole brains were obtained from wild-type mice at 8 and 24 weeks of age (6 animals/group), and the cortex and hippocampus were

https://doi.org/10.1016/j.heliyon.2018.e00601

dissected. Brain homogenates were prepared in NET-N buffer [20 mM Tris-HCl pH 8.0, 150 mM NaCl, 1 mM EDTA, 0.5% NP-40, 10% glycerol, 10 mM NEM, and protease inhibitors (Complete, Sigma); 1 or 3 ml/100 mg tissue for cortex or hippocampus, respectively]. A part of homogenates was mixed with 2x sample buffer at a 1:1 ratio, and 15 μl of the homogenate-sample buffer mixture of each sample were subjected to the immunoblot analysis using anti-SUMO antibodies. Another portion of the homogenates was cleared by centrifugation at 17,000 xg for 10 min, supernatants were collected, and the protein concentration was measured by BCA protein assay (Thermo Scientific). Brain lysates (10 μg protein each) were subjected to immunoblot analysis for the detection of endogenous SENP1 and SENP2. For the comparison between wild-type and 5xFAD mice, cerebral hemispheres from female wild-type and 5xFAD mice at 24 weeks of age (4 animals/group) were obtained. Brain homogenates were prepared in Tris buffer [20 mM Tris-HCl pH 7.4, 250 mM sucrose, 1 mM EDTA, 1 mM EGTA, protease inhibitors (Complete, Sigma); 1 mM Na_3VO_4, 8 mM NaF] and mixed with 2x sample buffer at a 1:1 ratio. Then, 15 μl of the homogenate-sample buffer mixture of each sample was subjected to immunoblot analysis using anti-SENP antibodies.

2.5. Immunoblot analysis

Protein samples were separated by 8% SDS-PAGE and transferred to polyvinylidene difluoride (PVDF) membranes (Millipore, Billerica, MA, USA). The membranes were blocked with 5% skim milk in TBS-T (20 mM Tris-HCl [pH 7.6], 136 mM NaCl, and 0.1% Tween 20) and incubated with horseradish peroxidase (HRP)-conjugated antibodies in 0.5% skim milk and TBST for 2 h at room temperature (RT). The antibodies used were HRP-conjugated anti-HA (3F10) (1:2000, Roche Diagnostics, Indianapolis, IN, USA), HRP-conjugated anti-FLAG (M2) (1:5000, Sigma), and HRP-conjugated anti-actin (1:20000, A3854, Sigma). To detect GFP-tagged proteins, the membranes were incubated with an anti-GFP antibody (JL8) (1:2000, Clontech, Mountain View, CA, USA) overnight at 4 °C and an HRP-conjugated anti-mouse IgG antibody (1:2000, Cell Signaling Technology, Danvers, MA, USA) for 2 h at RT. For the detection of SENP and SUMO proteins, the membranes were incubated with an anti-SENP1 antibody (1 μg/ml, NB100-56405, Novusbio, Littleton, CO, USA), anti-SENP2 antibody (1:2000, AP1232, Abgent, San Diego, CA, USA), anti-SUMO1 antibody (1:2000, 4972, Cell Signaling Technology), or anti-SUMO2/3 antibody (1:2000, 4974, Cell Signaling Technology) overnight at 4 °C and HRP-conjugated anti-rabbit IgG antibody (1:2000, Cell Signaling Technology) for 2 h at RT. Bands were detected with an enhanced chemiluminescence reagent (Clarity Western ECL Substrate, Bio-Rad, Hercules, CA, USA) using an image analyzer (Pxi, Syngene, Cambridge, UK), and quantified using Gene Tools (Syngene).

https://doi.org/10.1016/j.heliyon.2018.e00601

2.6. Peptide competition of the anti-SENP1 antibody

Two sets of hippocampal lysates (10 μg protein) from female mice at 8 and 24 weeks of age were subjected to 8% SDS-PAGE. The proteins were transferred to a PVDF membrane and the membrane was cut in two, with both portions carrying the same set of samples. The anti-SENP1 antibody (NB100-56405, Novusbio) was diluted in buffer (TBST:PBS = 1:1) containing 0.5% bovine serum albumin (BSA) at 0.5 μg/ml. The immunizing peptide corresponding to amino acid 578−590 of human SENP1 (amino acid sequence: EFDTNGWQLFSKK) was synthesized by GenScript (Piscataway, NJ, USA). The peptide was dissolved in distilled water, and 10 μl of the peptide solution (2 μg/μl) or water was added to 2 ml of the antibody solution and incubated for 24 h at 4 °C with gentle agitation. After the membranes were blocked with 5% skim milk in TBS-T, they were incubated with the antibody solution with or without peptide overnight at 4 °C followed by incubation with the secondary antibody and signal detection as described above.

2.7. Immunocytostaining

HEK293 cells (1×10^5 cells/well) were seeded into 4-well chamber slides (Thermo Fisher Scientific) and cotransfected with plasmids expressing FLAG-tagged APP, HA-tagged SUMO1/2, and His-tagged SENP by lipofection. The plasmid DNAs were mixed in a ratio of 3:1:1 for APP:SUMO:SENP. After 24 h of transfection, the cells were fixed with 4% paraformaldehyde in PBS for 30 min at RT, permeabilized with 0.2% Triton X-100 for 10 min at RT, and blocked with 5% BSA in PBS for 1 h at RT. Then, the fixed cells were stained by specific primary antibodies in 1% BSA-PBS for 1.5 h at RT and secondary antibodies in 1% BSA-PBS for 1 h at RT. The antibodies used were an anti-DYKDDDDK-tag rat monoclonal antibody (6F7) (1 μg/ml, Wako Pure Chemical Industries), anti-His mouse monoclonal antibody (2 μg/ml, D291, MBL, Nagoya, Japan), Alexa Fluor 555-conjugated goat anti-rat IgG antibody (1:500, Thermo Scientific), Alexa Fluor 594-conjugated goat anti-rat IgG antibody (1:500, Thermo Scientific), and DyLight 488-conjugated goat anti-mouse IgG antibody (1:500, Jackson Immuno Research). Cells were also counterstained with 4′, 6-diamidino-2-phenylindole (DAPI, AAT Bioquest). Cell images were obtained using a fluorescence microscope (IX83, Olympus, Tokyo, Japan) with a 40× objective lens and CellSens software (Olympus).

2.8. Reverse transcription quantitative polymerase chain reaction (RT-qPCR)

Mouse brains were obtained from 6 animals in each group. Total RNA was extracted from cerebral hemispheres with Isogen (Nippon Gene Co., Ltd, Toyama, Japan). First-strand cDNAs were synthesized using SuperScript VILO Master Mix (Thermo Fisher). The qPCR analysis was performed using KOD SYBR qPCR mix (Toyobo)

https://doi.org/10.1016/j.heliyon.2018.e00601

and the Applied Biosystems StepOne Real Time PCR system (Thermo Fisher). Primers used were SENP1, 5′-TGGGTGGAATAAACAACGAGGCCTGCAG GATCCTC-3′ and 5′-GCTGTCGATGGCAAAGGTTGGTCCCCCACACGCTC-3'; and SENP2, 5′-GAAATACAGATCTCAACCTCTTAGAGTGGACCCAC-3′ and 5′- ACACCTCTAGTCAGGGCCATTGTGGAGAGGCCTTC-3'. cDNA fragments amplified with the primers described above were subcloned into a pGEM-T vector and were used as standards.

2.9. Statistical analysis

The data are expressed as the mean ± SD. Comparisons among multiple groups were performed by one-way ANOVA followed by post hoc tests (Tukey's multiple comparison test). Comparisons between two groups were analyzed by t-test. Statistical analyses were performed in Prism5 (Graph Pad, La Jolla, CA, USA).

3. Results

3.1. Identification of SENP proteins that affect APP SUMOylation

To identify SENP proteins that affect APP SUMOylation, we analyzed SUMOylated APP in the presence or absence of SENP proteins. Cell lysates were obtained from cells co-expressing FLAG-tagged APP and His-tagged SENP proteins with HA-tagged SUMO1 or SUMO2, and APP was immunoprecipitated by the anti-FLAG antibody. Through the detection of SUMO1 using the anti-HA antibody, multiple SUMO1-conjugated APP bands larger than 100 kDa in size were observed in the absence of SENP (Fig. 1A). The intensity of SUMO1-conjugated APP bands at the size of approximately 130 kDa and larger was decreased in the presence of SENP1 and SENP2 but not SENP3 (Fig. 1A). A band at an approximate size of 110 kDa remained in the presence of SENP1 and SENP2, thus suggesting that one or more SUMOylation sites are resistant to these enzymes. With SUMO2 co-expression, multiple SUMO2-conjugated APP bands were observed in the vector control condition, and the intensity of these bands was decreased by SENP1 and SENP2 but not SENP3 (Fig. 1B). Though the expression levels of APP in input samples seemed slightly different among the samples, the amounts of APP in the IP samples appeared to be more similar, which means that the immunoprecipitation efficiency was similar among the samples. These results suggest that the decrease in the SUMO-modified APP bands in the presence of SENP1 and SENP2 in the IP samples was attributed to the reduced amount of SUMOylated APP.

In the input samples, the anti-HA antibody detected a reduced amount of SUMOylated proteins in the presence of SENP proteins with SUMO2 but not SUMO1 co-expression (Fig. 1A, B). In addition, we could not clearly detect SENP proteins using

https://doi.org/10.1016/j.heliyon.2018.e00601

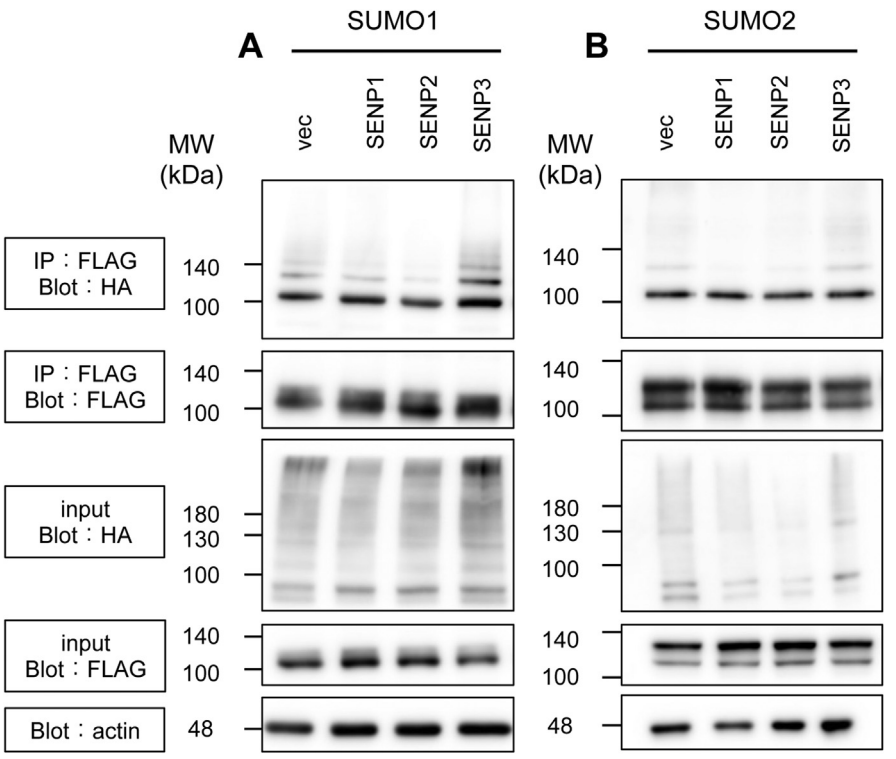

Fig. 1. Effects of SENP proteins in APP SUMOylation. HEK293 cells were cotransfected with plasmids expressing FLAG-tagged APP, HA-tagged SUMO1 (A) or SUMO2 (B), and His-tagged SENP1, 2, 3 or empty vector (vec). The cell lysates were immunoprecipitated with an anti-FLAG M2 antibody. Immunoprecipitate (IP) and input lysate (input) samples were applied for immunoblotting with anti-HA, anti-FLAG, and anti-β-actin antibodies. The full, uncropped images are available as Supplementary Fig. 1.

the anti-His-tag antibody in either condition. Therefore, we performed the same experiment using EGFP-fused SENP proteins (Fig. 2). Cell lysates were obtained from cells co-expressing FLAG-tagged APP and EGFP-fused SENP proteins with HA-tagged SUMO1 or SUMO2. APP was immunoprecipitated by the anti-FLAG antibody and SUMO-conjugated APP was detected by anti-HA antibody. The result was essentially the same as that in Fig. 1. In conditions of both SUMO1 and SUMO2 co-expression, poly-SUMOylated APPs at a size of approximately 130 kDa and larger were observed in the vector control condition, and the amount was reduced in the presence of SENP1 and SENP2 but not SENP3 (Fig. 2). Inconsistent with the result using His-tagged SENPs (Fig. 1), a large amount of mono-SUMOylated APP was immunoprecipitated in this condition using EGFP-fused SENPs. Though the expression levels of FLAG-tagged APP in the input were different among the samples, the amounts of immunoprecipitated APP detected by the anti-FLAG antibody were similar. Quantitative analysis showed that the levels of mono-SUMOylated APP were not affected by SENPs (Fig. 2C), but poly-SUMOylated APP levels were significantly reduced by SENP1 and SENP2 but not SENP3 (Fig. 2D). In the examination of SENP protein expression, we were able to clearly detect all SENPs with the anti-GFP antibody. Consistently, the global SUMOylation

https://doi.org/10.1016/j.heliyon.2018.e00601

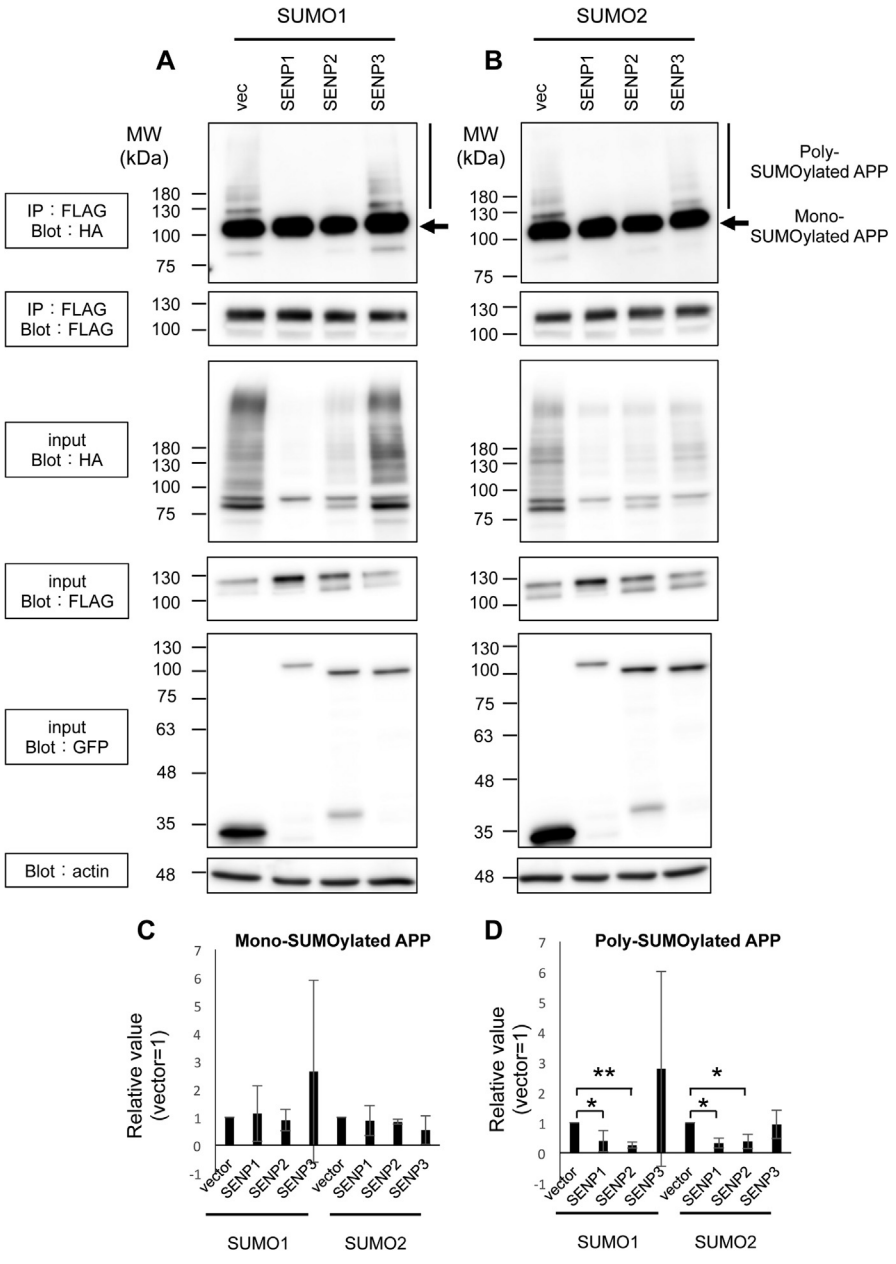

Fig. 2. Effects of EGFP-fused SENP proteins in APP SUMOylation. HEK293 cells were cotransfected with plasmids expressing FLAG-tagged APP, HA-tagged SUMO1 (A) or SUMO2 (B), and EGFP-fused SENP1, 2, 3 or empty vector (vec). The cell lysates were immunoprecipitated with an anti-FLAG M2 antibody. Immunoprecipitate (IP) and input lysate (input) samples were applied for immunoblotting with anti-HA, anti-FLAG, anti-GFP, and anti-β-actin antibodies. The experiment was repeated three times and representative results are shown. The full, uncropped images are available as Supplementary Fig. 2. The band intensities of polySUMOylated APP (indicated by bars), mono-SUMOylated APP (indicated by arrows) in anti-HA blots, and APP in anti-FLAG blots were quantified, and the values of poly- and mono-SUMOylated APP were normalized by the value of APP detected by the anti-FLAG antibody. The calculated values were normalized by the value of the vector control sample and the means and SDs of 3 independent experiments are presented (C, D). The results of the t-tests are indicated as *$p < 0.05$ and **$p < 0.01$.

https://doi.org/10.1016/j.heliyon.2018.e00601

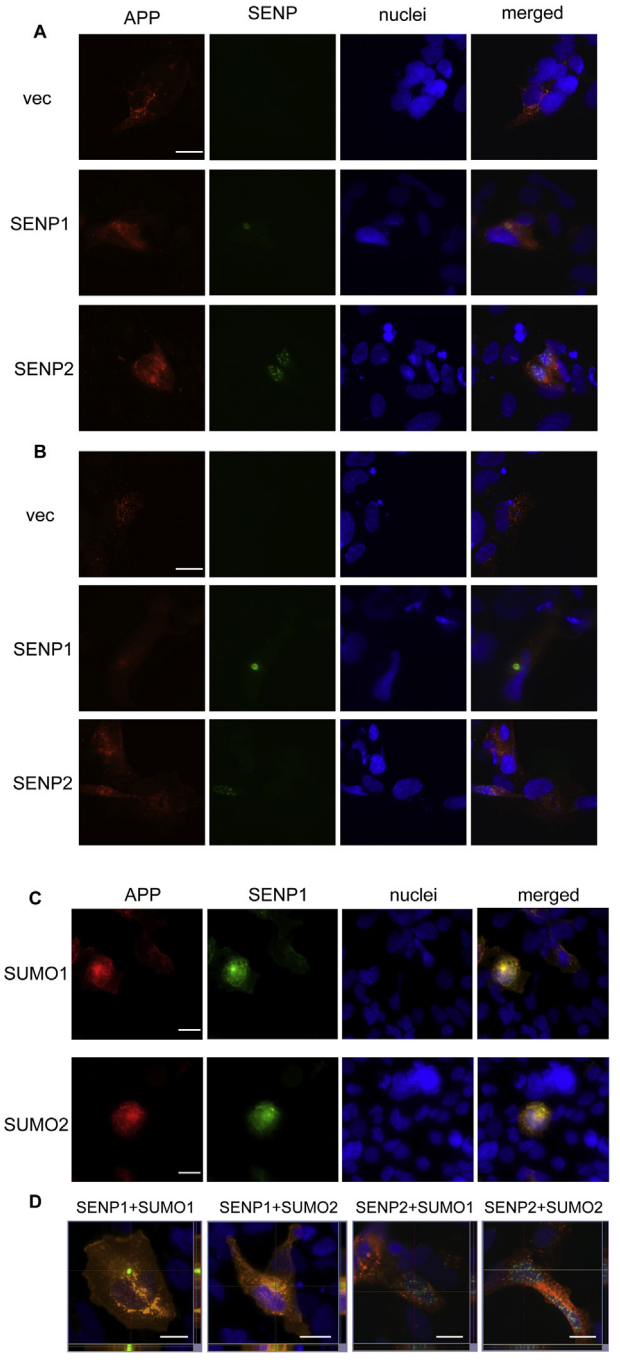

Fig. 3. Intracellular localization of APP and SENP proteins. A, B. HEK293 cells were cotransfected with plasmids expressing FLAG-tagged APP, HA-tagged SUMO1 (A) or SUMO2 (B), and His-tagged SENP1, 2, or empty vector (vec). Fixed cells were immunostained with anti-DYKDDDDK, anti-His, Alexa Fluor 555-conjugated anti-rat IgG and DyLight 488-conjugated anti-mouse IgG antibodies, and then counterstained with DAPI. The bar in the upper left panel indicates 20 μm. C. HEK293 cells were cotransfected with plasmids expressing FLAG-tagged APP, HA-tagged SUMO1 or SUMO2, and His-tagged SENP1. Fixed cells were immunostained with anti-DYKDDDDK, anti-His, Alexa Fluor 594-conjugated anti-rat IgG antibody and DyLight 488-conjugated anti-mouse IgG antibodies, and

https://doi.org/10.1016/j.heliyon.2018.e00601

detected by the anti-HA antibody was reduced by SENP1 and SENP2 in the input samples. The global SUMOylation by SUMO2 was also reduced by SENP1, SENP2 and SENP3. These results indicate that overexpressed SENP proteins functioned as deSUMOylating enzymes. Taken together, these results suggest that SENP1 and SENP2 reduced the modification of APP by SUMO1 and SUMO2.

3.2. Intracellular localization of APP and SENP proteins

We next examined the intracellular localization of SENPs and APP (Fig. 3). Cells were co-transfected with plasmids expressing FLAG-tagged APP and His-tagged SENP with HA-tagged SUMO1 or SUMO2. APP labeled by Alexa Fluor 555 was observed outside of the nucleus in both the vector control and SENP co-expression conditions. No significant differences were observed between SUMO1-coexpressing (Fig. 3A) and SUMO2-coexpressing (Fig. 3B) cells. SENP1 was expressed throughout the cell at a low level and occasionally condensed into a round vesicle-like structure outside of the nucleus (Fig. 3A, B). These results were reproduced with the use of secondary antibodies whose labeled fluorocromes had less spectral overlap, i.e., Alexa Fluor 594 and DyLight 488 (Fig. 3C). A similar pattern of SENP1 localization outside of the nucleus has been reported in other cells [23, 24], although the expression of SENP1 has previously been demonstrated to be primarily in the nucleus [25]. APP was found to overlap with SENP1 located outside of the nucleus, but Z-stack analysis revealed that APP was not concentrated in the SENP1-positive vesicle-like structure (Fig. 3D). In contrast, SENP2 was mainly expressed in the nucleus where APP was not observed (Fig. 3A, D). No significant differences were observed between SUMO1- and SUMO2-coexpressing cells (Fig. 3A, B, D). We analyzed 29 to 43 cells of each condition in detail and found that all cells were stained in the similar manner as presented in the figure.

3.3. Expression of SENP1 and SENP2 transcripts in mouse brains

Limited information is available in mice regarding SUMOylation-regulating proteins. Therefore, we analyzed the mRNA levels of deSUMOylation enzymes SENP1 and SENP2 by qPCR in the brains of wild-type mice at 8, 16, and 24 weeks of age. The SENP1 mRNA levels in female mice increased in an age-dependent manner, and a significant difference was detected in the levels between 8 and 24 weeks, whereas no changes were observed in male mice (Fig. 4A). The levels of SENP2 mRNA did not change in either male or female mice (Fig. 4B). These results are indicative of a sex difference in the expression of SENP1 but not SENP2.

then counterstained with DAPI. The bar in the left panels indicates 20 μm. D. The merged Z-stack images were obtained from cells in the experiments of Fig. 3C (SENP1) and Fig. 3A, B (SENP2). The images are composed of 10 Z-stack images in 0.35-μm intervals. The bar in each panel indicates 20 μm.

https://doi.org/10.1016/j.heliyon.2018.e00601

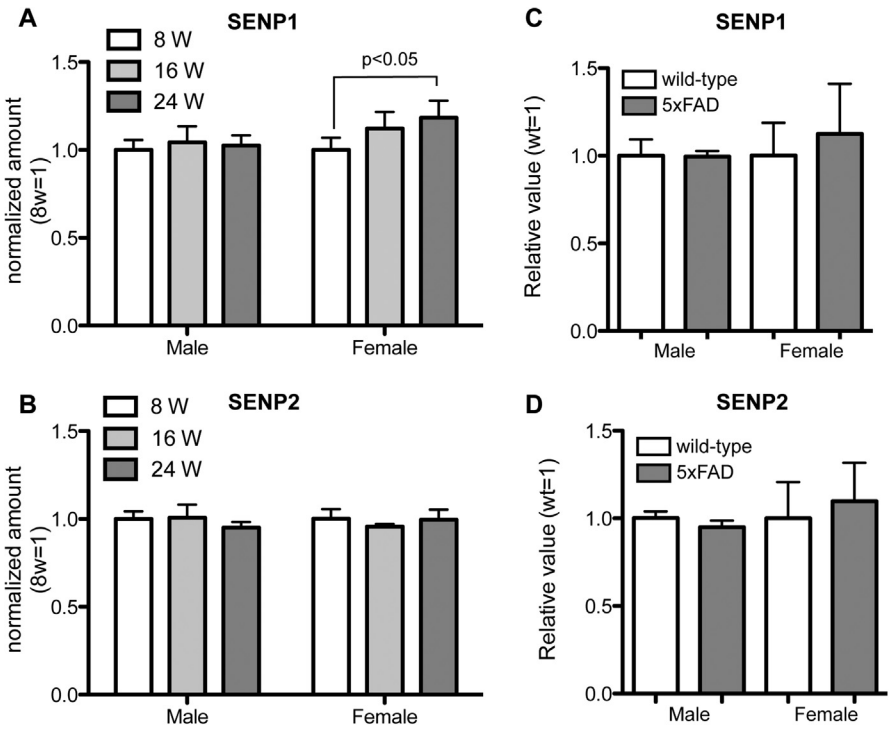

Fig. 4. Quantitative analysis of SENP transcripts in the mouse brain. Quantitative PCR analysis was performed with total RNA from the mouse brain. RNA samples from wild-type mice at 8, 16, and 24 weeks of age (A, B) and wild-type and 5xFAD mice at 24 weeks of age (C, D) were analyzed. The relative values of SENP1 (A, C) and SENP2 (B, D) transcripts normalized to those at 8 weeks (A, B) or those in wild-type mice (C, D) are shown as the mean ± SD. The number of samples in each group is 6. The P-value of a one-way ANOVA is shown.

We next compared SENP transcription levels between wild-type and 5xFAD mice, an Aβ overexpression AD mouse model [19], at 24 weeks of age. No differences in SENP1 expression (Fig. 4C) or SENP2 expression (Fig. 4D) were detected between the two groups in either sex. In female, one sample out of six showed an extreme value in both wild-type and 5xFAD groups. We did not exclude them because we found no specific reason. When these values are excluded the results would show the smaller SD values, which are comparable to the male's results and statistically reliable [SENP1 ($n = 5$): wild-type 1.00 ± 0.09, 5xFAD 1.09 ± 0.14; SENP2 ($n = 5$): wild-type 1.00 ± 0.14, 5xFAD 1.10 ± 0.15].

3.4. Protein levels of SENP1 and SENP2 in mouse brains

To verify the findings in transcript levels of SENP1 and SENP2, we analyzed the protein levels of these enzymes in mouse brains. Brain lysates from the cortex and hippocampus of 8- and 24-week-old mice were subjected to immunoblot analysis using anti-SENP1 and SENP2 antibodies (Fig. 5). The anti-SENP1 antibody detected multiple bands in lysates from both the cortex and hippocampus (Fig. 5A). To confirm the specificity of the antibody, we performed a blocking assay using the

https://doi.org/10.1016/j.heliyon.2018.e00601

immunizing peptide of the polyclonal antibody. The antibody was pre-incubated with or without the blocking peptide and used for the immunoblot analysis (Fig. 5B). All major bands detected by the antibody without the peptide were diminished in the blot using a neutralized antibody, suggesting that these bands represented the SENP1 protein. Two bands approximately 75 kDa in size (designated bands [a] in Fig. 5A, B) were full-length SENP1 according to a previous report [26], and the bands smaller than 75 kDa are likely the cleaved products of SENP1. In female, the levels of full-length SENP (bands [a]) were similar between the two age groups in both the cortex and hippocampus (Fig. 5C). Interestingly, the intensity of the smallest band at approximately 30 kDa in size (band [b] in Fig. 5A, B) was significantly greater in 24-week-old mice than in 8-week-old mice in both the cortex and hippocampus (Fig. 5D). These results suggest that the total SENP1 protein level was likely greater in 24-week-old female mice than in 8-week-old female mice. On the other hand, in male mice, although the intensity of the smallest band (band [b]) increased the cortex, it is not in the hippocampus (Fig. 5D), and the intensity of the full-length SENP1 bands (bands [a]) slightly but significantly decreased with age in the cortex (Fig. 5C). Thus, the total SENP1 level may not be largely different between the two ages. These findings suggest that the SENP1 increased with age in female but not in male mice also in protein level.

We also analyzed SENP2 protein expression in the cortex and hippocampus of male and female mouse brains at 8 and 24 weeks of age (Fig. 5E, F). The SENP2 band was detected at approximately 63 kDa (Fig. 5E). Quantitative analysis showed no significant difference between age groups in SENP2 expression in the cortex and hippocampus of both male and female mice (Fig. 5F), which is consistent with the results of SENP2 transcript expression (Fig. 4B).

To examine the effect of amyloid burden on SENP1 and SENP2 expression, we compared SENP protein levels and protein SUMOylation between wild-type and 5xFAD mice at 24 weeks of age. No significant difference was observed in the levels of endogenous SENP1 or SENP2 between the cerebral homogenates from wild-type and 5xFAD mice (Fig. 5G, H). These results were consistent with the levels of SENP1 and SENP2 transcripts (Fig. 4C, D).

3.5. Global protein SUMOylation in wild-type mouse brains

To examine whether change in the expression levels of SENP proteins influences global SUMOylation in mouse brains, we performed immunoblot analyses using anti-SUMO1 and SUMO2/3 antibodies. The anti-SUMO1 antibody showed no noticeable difference in the band patterns between 8 and 24 weeks of age in either the cortex or hippocampus in either sex (Fig. 6A). Quantitative analysis confirmed that no significant difference was detected between the age groups (Fig. 6B). Similarly, no significant difference was observed in the SUMOylated bands detected by

https://doi.org/10.1016/j.heliyon.2018.e00601

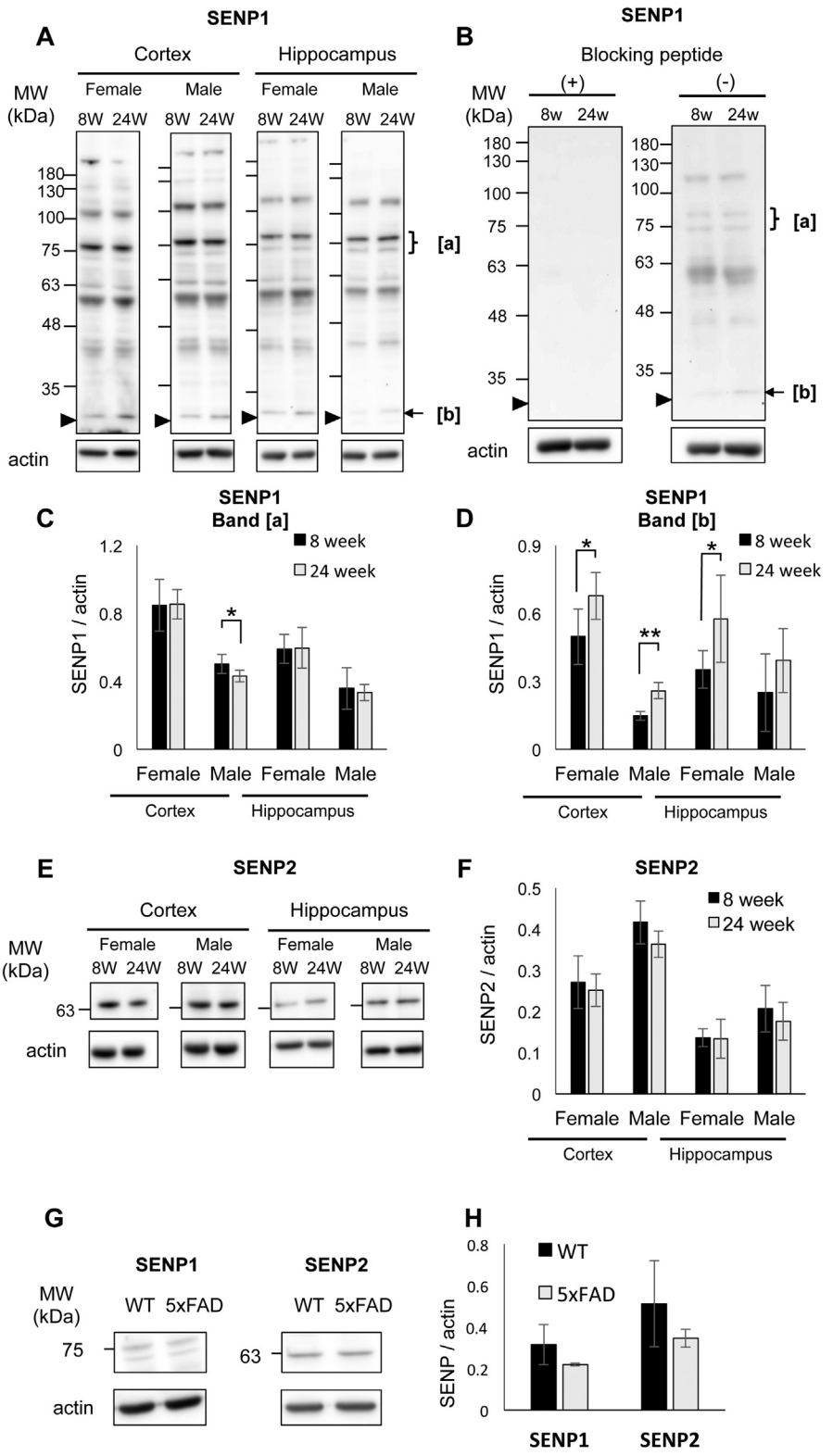

Fig. 5. Expression of SENP proteins in the mouse brain. Lysates from the cortex and hippocampus of wild-type mice at 8 and 24 weeks of age were subjected to immunoblot analysis using anti-SENP1

https://doi.org/10.1016/j.heliyon.2018.e00601

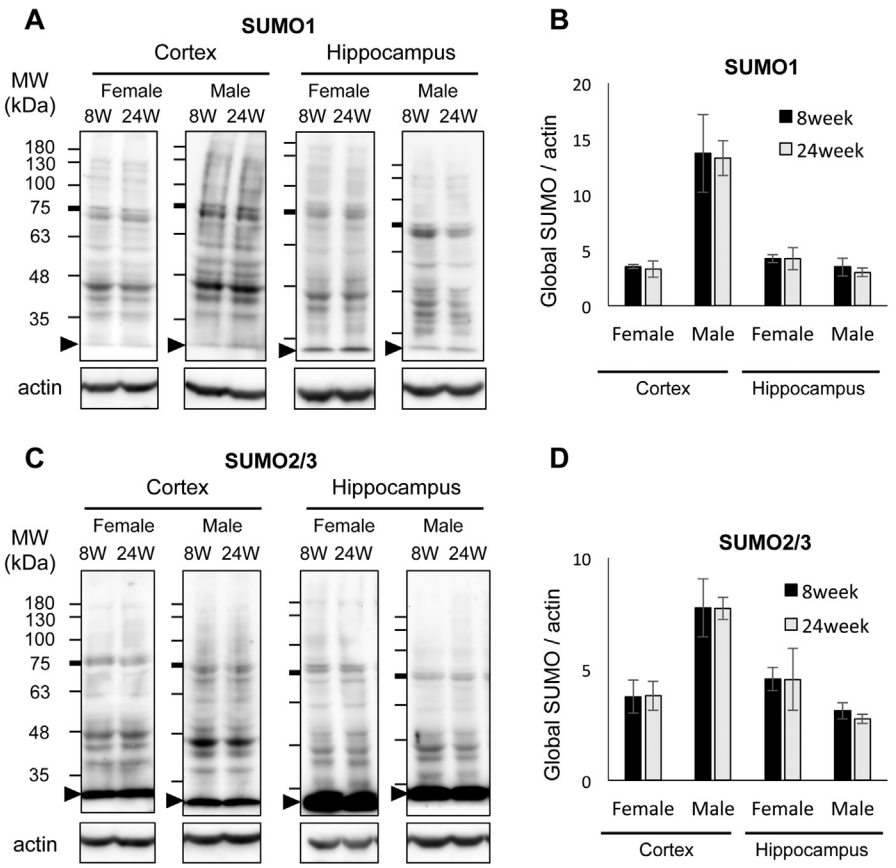

Fig. 6. Global protein SUMOylation in the wild-type mouse brain. Homogenates from the cortex and hippocampus of wild-type mice at 8 and 24 weeks of age were subjected to the immunoblot analysis using anti-SUMO1 (A upper panels), anti-SUMO2/3 (C upper panels), and anti-β-actin (lower panels) antibodies. Representative results of the SUMO1 (A) and SUMO2/3 (C) immunoblots are shown. Arrowhead indicates the position of the dye front of each gel. The intensities of bands between 180 kDa and 35 kDa in size in A and C were measured and normalized by the values of β-actin (B, D). The number of animals in each group was 4. The full, uncropped images of A and C are available as Supplementary Figs. 6 and 7, respectively.

(A, B upper panels), anti-SENP2 (E upper panels), and anti-β-actin (lower panels) antibodies. A. Representative results of the SENP1 immunoblots are shown. B. Blots of hippocampal lysates from female mice at 8 and 24 weeks of age were incubated with the anti-SENP1 antibody with (+) or without (-) blocking peptide. Arrowhead indicates the position of the dye front of each gel. C, D. The intensities of SENP1 bands indicated as [a] and [b] in A were measured and normalized by the values of β-actin. The number of animals used in each group was 6. E. Representing results of SENP2 immunoblots are shown. F. The intensities of SENP2 bands in D were measured and normalized by the values of β-actin. The number of animals used in each group was 6. G, H. Homogenates from the cortex and hippocampus of wild-type and 5xFAD mouse brains at 24 weeks of age were subjected to immunoblot analysis using anti-SENP1 and anti-SENP2 antibodies (G upper panels), and anti-β-actin (G lower panels) antibodies. The intensities of bands in G were measured and normalized by the values of β-actin (B, D). The number of animals in each group was 4. The full, uncropped images of A, B, E and G are available as Supplementary Figs. 3A, B, 4, and 5 respectively.

https://doi.org/10.1016/j.heliyon.2018.e00601

the anti-SUMO2/3 antibody in either the cortex or hippocampus in either sex (Fig. 6C, D). These results suggest that the change in the SENP1 expression levels did not influenced global SUMOylation in the mouse brain. Global SUMOylation is the final outcome of the regulation by multiple de-SUMOylating enzymes and SUMO E3 ligases. Thus, the lack of an effect on the SUMOylation of all proteins caused by a change in just one of these enzymes is not surprising. Ficulle et al. also showed that the age-dependent change in SENP1 expression levels did not correlate with global SUMOylation [27].

4. Discussion

In this study, we found that SENP1 and SENP2 decreased both the SUMO1 and SUMO2 modification of APP (Figs. 1 and 2). APP was observed to overlap with the extranuclear localization of SENP1 (Fig. 3). Thus, SENP1 may have a chance to interact with APP to remove SUMO1 and SUMO2 from APP. Interestingly, although SENP2 was observed only in the nucleus (Fig. 3), SENP2 was able to reduce the SUMOylation of APP to a level comparable to that in SENP1-expressing cells (Figs. 1 and 2). As SENP2 can shuttle between the cytoplasm and the nucleus [28], one possible interpretation is that an undetectable level of SENP2 in the cytoplasm may be sufficient for the deSUMOylation of APP.

Quantitative PCR and immunoblot analyses showed no difference in SENP1 levels between wild-type and 5xFAD mice (Fig. 4C). These results were consistent with previous studies reporting that similar SENP1 mRNA expression was observed between wild-type and Tg2576 AD model mice at both 1.5 and 6 months of age [29] and that similar SENP1 protein levels were detected in the hippocampus, cortex and cerebellum of wild-type and Tg2576 AD model mice at 9 months of age [26]. On the other hand, SENP1 mRNA expression increased in an age-dependent manner only in female mice (Fig. 4A). Thus, SENP1 expression was presumed to increase in an age-dependent manner in female AD model mice, as observed in wild-type mice (Figs. 4A and 5A). Furthermore, amyloid pathology is likely to affect SENP1 expression, although Aβ production and plaque formation have been shown to age-dependently increase in these model mice. Amyloid pathology occurs at an earlier age and progresses more aggressively in female mice than in male mice in AD mouse models [18, 30, 31]. In 5xFAD mice, the amount of β-secretase-cleaved fragments in females was significantly higher than that in males at 6 months of age [30]. The SUMOylation sites in APP are close to a β-secretase cleavage site, and APP SUMOylation decreases the production of Aβ *in vitro* [16], thus suggesting that SUMO modification interferes with the β-cleavage. Increased SENP1 expression may contribute to the increase in Aβ by decreasing the SUMOylation of APP. Together, our results suggest that the age-dependent increase in SENP1 expression may contribute to the rapid progression of amyloid pathology in female mice.

https://doi.org/10.1016/j.heliyon.2018.e00601

5. Conclusion

We found that SENP1 and SENP2 promote deSUMOylation of APP and that SENP1 expression increases in an age-dependent manner only in female mice. Our findings provide a clue to understanding the sex difference in amyloid pathology in AD.

Declarations

Author contribution statement

Takuma Maruyama: Performed the experiments; Analyzed and interpreted the data; Wrote the paper.

Yoichiro Abe, Takako Niikura: Conceived and designed the experiments; Performed the experiments; Analyzed and interpreted the data; Contributed reagents, materials, analysis tools or data; Wrote the paper.

Funding statement

This research did not receive any specific grant from funding agencies in the public, commercial, or not-for-profit sectors.

Competing interest statement

The authors declare no conflict of interest.

Additional information

Supplementary content related to this article has been published online at https://doi.org/10.1016/j.heliyon.2018.e00601.

References

[1] J.M. Henley, T.J. Craig, K.A. Wilkinson, Neuronal SUMOylation: mechanisms, physiology, and roles in neuronal dysfunction, Physiol. Rev. 94 (2014) 1249−1285.

[2] R.T. Hay, SUMO: a history of modification, Mol. Cell. 18 (2005) 1−12.

[3] A. Nayak, S. Müller, SUMO-specific proteases/isopeptidases: SENPs and beyond, Genome Biol. 15 (2014) 422.

[4] T. Yamaguchi, P. Sharma, M. Athanasiou, A. Kumar, S. Yamada, M.R. Kuehn, Mutation of SENP1/SuPr-2 reveals an essential role for desumoylation in mouse development, Mol. Cell. Biol. 25 (2005) 5171−5182.

[5] X. Kang, Y. Qi, Y. Zuo, Q. Wang, Y. Zou, R.J. Schwartz, J. Cheng, E.T.H. Yeh, SUMO-specific protease 2 is essential for suppression of polycomb group protein-mediated gene silencing during embryonic development, Mol. Cell. 38 (2010) 191−201.

[6] H. Zhang, Y. Wang, A. Zhu, D. Huang, S. Deng, J. Cheng, M.X. Zhu, Y. Li, SUMO-specific protease 1 protects neurons from apoptotic death during transient brain ischemia/reperfusion, Cell Death Dis. 7 (2016) e2484.

[7] J. Fu, H.M.I. Yu, S.Y. Chiu, A.J. Mirando, E.O. Maruyama, J.G. Cheng, W. Hsu, Disruption of SUMO-specific protease 2 induces mitochondria mediated neurodegeneration, PLoS Genet. 10 (2014).

[8] L. Schorova, S. Martin, Sumoylation in synaptic function and dysfunction, Front. Synaptic Neurosci. 8 (2016).

[9] J.S. Steffan, N. Agrawal, J. Pallos, E. Rockabrand, L.C. Trotman, N. Slepko, K. Illes, T. Lukacsovich, Y.-Z. Zhu, E. Cattaneo, P.P. Pandolfi, L.M. Thompson, J.L. Marsh, SUMO modification of Huntingtin and Huntington's disease pathology, Science 304 (2004) 100−104.

[10] E. Fei, N. Jia, M. Yan, Z. Ying, Q. Sun, H. Wang, T. Zhang, X. Ma, H. Ding, X. Yao, Y. Shi, G. Wang, SUMO-1 modification increases human SOD1 stability and aggregation, Biochem. Biophys. Res. Commun. 347 (2006) 406−412.

[11] T. Niikura, Y. Kita, Y. Abe, SUMO3 modification accelerates the aggregation of ALS-Linked SOD1 mutants, PLoS One 9 (2014).

[12] Y. Li, H. Wang, S. Wang, D. Quon, Y.-W. Liu, B. Cordell, Positive and negative regulation of APP amyloidogenesis by sumoylation, Proc. Natl. Acad. Sci. U. S. A. 100 (2003) 259−264.

[13] V. Dorval, P.E. Fraser, Small ubiquitin-like modifier (SUMO) modification of natively unfolded proteins tau and α-synuclein, J. Biol. Chem. 281 (2006) 9919−9924.

[14] J.B. Hoppe, C.G. Salbego, H. Cimarosti, SUMOylation: novel neuroprotective approach for Alzheimer's disease? Aging Dis. 6 (2015) 322.

[15] L. Lee, M. Sakurai, S. Matsuzaki, O. Arancio, P. Fraser, SUMO and alzheimer's disease, Neuromolecular Med. 15 (2013) 720−736.

[16] Y.Q. Zhang, K.D. Sarge, Sumoylation of amyloid precursor protein negatively regulates A?? aggregate levels, Biochem. Biophys. Res. Commun. 374 (2008) 673−678.

https://doi.org/10.1016/j.heliyon.2018.e00601

[17] C.J. Pike, Sex and the development of Alzheimer's disease, J. Neurosci. Res. 95 (2017) 671–680.

[18] C. Hirata-Fukae, H.F. Li, H.S. Hoe, A.J. Gray, S.S. Minami, K. Hamada, T. Niikura, F. Hua, H. Tsukagoshi-Nagai, Y. Horikoshi-Sakuraba, M. Mughal, G.W. Rebeck, F.M. LaFerla, M.P. Mattson, N. Iwata, T.C. Saido, W.L. Klein, K.E. Duff, P.S. Aisen, Y. Matsuoka, Females exhibit more extensive amyloid, but not tau, pathology in an Alzheimer transgenic model, Brain Res. 1216 (2008) 92–103.

[19] H. Oakley, S.L. Cole, S. Logan, E. Maus, P. Shao, J. Craft, A. Guillozet-Bongaarts, M. Ohno, J. Disterhoft, E.L. Van, R. Berry, R. Vassar, Intraneuronal beta-amyloid aggregates, neurodegeneration, and neuron loss in transgenic mice with five familial Alzheimer's disease mutations: potential factors in amyloid plaque formation, J. Neurosci. 26 (2006) 10129–10140.

[20] L. Devi, M.J. Alldred, S.D. Ginsberg, M. Ohno, Sex- and brain region-specific acceleration of β-amyloidogenesis following behavioral stress in a mouse model of Alzheimer's disease, Mol. Brain 3 (2010).

[21] J. Cheng, X. Kang, S. Zhang, E.T.H. Yeh, SUMO-specific protease 1 is essential for stabilization of HIF1?? during hypoxia, Cell 131 (2007) 584–595.

[22] L. Gong, E.T.H. Yeh, Characterization of a family of nucleolar SUMO-specific proteases with preference for SUMO-2 or SUMO-3, J. Biol. Chem. 281 (2006) 15869–15877.

[23] I. Meinecke, A. Cinski, A. Baier, M.A. Peters, B. Dankbar, A. Wille, A. Drynda, H. Mendoza, R.E. Gay, R.T. Hay, B. Ink, S. Gay, T. Pap, Modification of nuclear PML protein by SUMO-1 regulates Fas-induced apoptosis in rheumatoid arthritis synovial fibroblasts, Proc. Natl. Acad. Sci. U. S. A. 104 (2007) 5073–5078.

[24] E. Foran, L. Rosenblum, A. Bogush, P. Pasinelli, D. Trotti, Sumoylation of the astroglial glutamate transporter EAAT2 governs its intracellular compartmentalization, Glia 62 (2014) 1241–1253.

[25] D. Bailey, P. O'Hare, Characterization of the localization and proteolytic activity of the SUMO-specific protease, SENP1, J. Biol. Chem. 279 (2004) 692–703.

[26] L.E. McMillan, J.T. Brown, J.M. Henley, H. Cimarosti, Profiles of SUMO and ubiquitin conjugation in an Alzheimer's disease model, Neurosci. Lett. 502 (2011) 201–208.

https://doi.org/10.1016/j.heliyon.2018.e00601

[27] E. Ficulle, M.D.S. Sufian, C. Tinelli, M. Corbo, M. Feligioni, Aging-related SUMOylation pattern in the cortex and blood plasma of wild type mice, Neurosci. Lett. 668 (2018) 48−54.

[28] Y. Itahana, E.T.H. Yeh, Y. Zhang, Nucleocytoplasmic shuttling modulates activity and ubiquitination-dependent turnover of SUMO-specific protease 2, Mol. Cell. Biol. 26 (2006) 4675.

[29] R. Nistico, C. Ferraina, V. Marconi, F. Blandini, L. Negri, J. Egebjerg, M. Feligioni, Age-related changes of protein SUMOylation balance in the A beta PP Tg2576 mouse model of Alzheimer's disease, Front. Pharmacol. 5 (2014).

[30] K.R. Sadleir, W.A. Eimer, S.L. Cole, R. Vassar, Aβ reduction in BACE1 heterozygous null 5XFAD mice is associated with transgenic APP level, Mol. Neurodegener. 10 (2015) 1.

[31] M.J. Callahan, W.J. Lipinski, F. Bian, R.A. Durham, A. Pack, L.C. Walker, Augmented senile plaque load in aged female beta-amyloid precursor protein-transgenic mice, Am. J. Pathol. 158 (2001) 1173−1177.

 https://doi.org/10.1016/j.heliyon.2018.e00601